

# Atom wave diffraction in an accelerating potential

**Timothy M Roach**

Physics Department, The College of the Holy Cross, Worcester, MA 01610, USA

E-mail: troach@holycross.edu

Received 2 June 2004

Published 24 August 2004

Online at [stacks.iop.org/JPhysB/37/3551](http://stacks.iop.org/JPhysB/37/3551)

doi:10.1088/0953-4075/37/17/010

## Abstract

Gravity or other accelerating potentials can significantly affect the visibility of fringes in atomic wave diffraction experiments. We examine several geometries in which laser-cooled atoms from a magneto-optic trap are accelerated into a diffraction grating and calculate how the thermal longitudinal momentum spread broadens the diffracted atomic beams. We find that the relative broadening typically depends upon the ratio of the thermal momentum to the momentum gained from acceleration. We show how large accelerations can thus be used to improve the fringe visibility and we apply our results to geometries used recently by other research groups.

## 1. Introduction

The development of laser-cooled atomic sources has opened up the interesting realm in which the mean thermal energy of an atom may be less than the gravitational potential energy due to even a 1 mm change in height. Experiments in atom optics are therefore often dramatically dependent upon the effects of gravity. Some atom interferometry experiments have made use of this to measure the local value of  $g$  with extreme precision [1]. Other experiments have made use of gravity as part of a confining potential to trap cold atoms [2, 3]. Gravity can also be used to accelerate the atoms in order to deliver them to an atom-optic element such as a mirror [4] or grating [5]. In our laboratory we are using atoms from a magneto-optic trap (MOT) to investigate matter-wave diffraction from a reflection mode diffraction grating made from a microscopic pattern of permanent magnetization written on a magnetic disc. In this paper we investigate how the resolvability of diffracted atomic waves depends upon the effects of accelerating potentials such as gravity.

We consider generally the diffraction of matter waves from a diffraction grating at normal incidence without regard for the details of the atom–grating interaction [5, 6]. In the absence of external potentials, constructive interference occurs at angles given by  $\sin \theta = n\lambda/d$ , where  $d$  is the grating spacing,  $\lambda$  is the atomic deBroglie wavelength and  $n$  is an integer. An applied potential will cause the atoms to accelerate, so that the atomic wavelength becomes a function

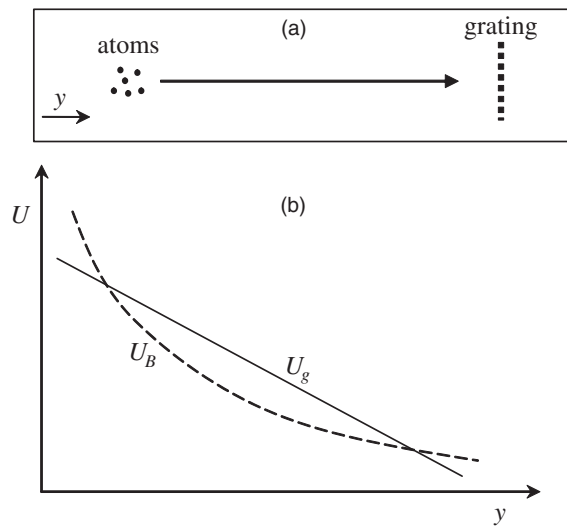


**Figure 1.** (a) Cloud of atoms accelerated towards a grating. (b) Possible accelerating potentials due to either gravity or magnetic field.

of position, and will make the atoms move in curved trajectories, so that angle is no longer a useful parameter.

The cloud of atoms collected by a MOT has a thermal momentum distribution and a Gaussian spatial distribution. In the language of optics, these distributions represent a source with a range of wavelengths, an angular spread, a non-zero spatial extent and non-zero depth of field. Each of these elements can contribute to a broadening of the subsequently diffracted atomic beams. The transverse momentum and transverse spatial distributions are often the dominant broadening factors, and apertures or focusing elements are sometimes used to reduce their effects. If these have been sufficiently reduced, one finds that the longitudinal momentum distribution remains a source of broadening. We consider in this paper only the effect of the momenta along the direction normal to the grating surface (the 1D longitudinal momentum distribution), and we model the atomic cloud as a point source with a temperature  $T$ . For other types of cold-atom sources, such as a cooled beam [7] or a continuous extraction MOT [8], a slight modification of the initial momentum distribution is needed in order to apply our results. For a standard MOT, in order to transfer the atoms to the surface, they must be pushed towards the grating (figure 1(a)). The atoms could, in principle, be released from the trap and simply be allowed to ballistically expand until they reach the grating surface, but this is not efficient nor is it possible in the presence of gravity, which will accelerate them.

A similar effect can be obtained by allowing the atoms to ‘fall’ in the gradient of a steady but non-uniform magnetic field. The potential energy of an atom with magnetic moment  $\mu$  due to the magnetic field  $\mathbf{B}$  is  $U_B = -\mu \cdot \mathbf{B} = -g_F m_F \mu_B B$ , where  $\mu_B$  is the Bohr magneton,  $g_F$  is the gyromagnetic ratio and  $m_F$  is the magnetic sublevel. As long as the atom remains in the original magnetic sublevel (the adiabatic approximation), the potential energy depends only upon the magnitude of the magnetic field. In this case,  $\mathbf{F}_B = -\nabla U_B = g_F m_F \mu_B \nabla(B)$ , and this force can be used to push the atoms into the grating. More generally, we must include the gravitational force so the total force is  $\mathbf{F}_{\text{tot}} = -\nabla U_g - \nabla U_B$ . To give a sense of the relative sizes of these two forces, we note that for rubidium atoms (which we use in our experiments), the maximum possible value of  $g_F m_F$  is 1, and in this case the two forces are equal if the

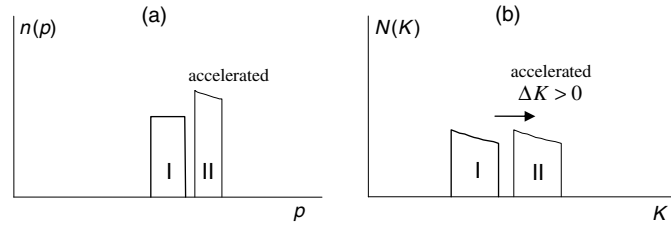


**Figure 2.** (a) A simple momentum distribution (I) and the resultant distribution (II) after acceleration through a fixed potential difference. The accelerated distribution is noticeably narrower. (b) These same distributions mapped onto the kinetic energy axis.

magnetic gradient is about  $14 \text{ Gauss cm}^{-1}$ . In general, the magnetic gradient will not be linear, and possible potential curves are illustrated in figure 1(b).

Regardless of the nature of the potential, there are common features to the motion of atoms within a non-uniform potential. We consider therefore a general potential  $U$ , the results of which can later be applied to specific cases. We assume that the potential is monotonically decreasing or increasing, so that the resultant force is always in one direction, and we model it as a 1D potential, dependent only upon  $y$ .

In this geometry an experiment in diffraction can be broken down into three parts, transport of atoms to the grating surface, diffraction from the grating and transport of the atoms to a detection region. The diffraction of an atom and its later trajectory both depend upon the momentum at the point of incidence upon the grating, so we begin by studying the evolution of the atomic momentum distribution when falling through the potential  $U(y)$ .

## 2. Incident momentum distribution

We define the longitudinal axis  $y$  with the atomic cloud initial position at  $y_0$  and the grating surface at a position  $y_G$ . If the potential decreases towards the grating then the atoms will be pushed into the grating. We refer to this as the ‘drop’ delivery method. Alternatively, if the potential increases then the atoms must be given an initial momentum to reach the grating; this we call the ‘launch’ delivery method. In our model all atoms begin at the same initial position and end at the same final position (the grating surface), so that the kinetic energy change  $\Delta K = U(y_0) - U(y_G)$  is the same for all atoms. To gain some understanding of the evolution of the momentum distribution we consider first a hypothetical rectangular momentum density distribution  $n(p)$  shown as line I in figure 2(a). Conservation of atoms in an infinitesimal portion of the distribution requires that

$$n(p) dp = N(K) dK \quad (1)$$

where  $N(K)$  is the distribution in  $K$ -space, and  $K = p^2/2M$ .

Using for convenience a mass  $M = 1$ ,

$$N(K) = n(p) \frac{dp}{dK} = n(p)/\sqrt{2K}. \quad (2)$$

This is curve I in figure 2(b). After an atom slides down the potential, its kinetic energy when incident upon the grating is  $K_i = K + \Delta K$  and the shifted distribution is shown as curve II in figure 2(b). We wish to find the corresponding incident momentum distribution  $n_i(p_i)$  so we begin with

$$n_i(p_i) = n(p) \frac{dp}{dp_i} \quad (3)$$

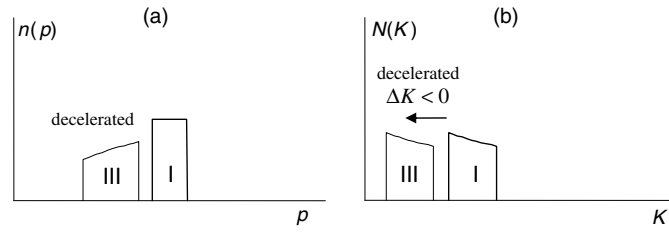


**Figure 3.** (a) Initial momentum distribution (I) and the resultant distribution (III) after deceleration through a fixed potential difference. The decelerated distribution is broadened. (b) These same distributions mapped onto the kinetic energy axis.

where  $p_i = \sqrt{p^2 + 2\Delta K}$  is the incident momentum. We find

$$n_i(p_i) = \frac{n(\sqrt{p_i^2 - 2\Delta K})}{\sqrt{1 - 2\Delta K/p_i^2}} \quad (4)$$

where the numerator is the original distribution evaluated at the original momentum.

This is shown as curve II in figure 2(a). Note that the accelerated distribution is narrowed compared to the original distribution. This is of advantage in resolving diffracted atoms, since the detected position spread is typically proportional to the incident momentum spread. If, on the other hand, we have an uphill gradient, then the atoms are slowed and the atomic distribution is broadened, as is shown in figure 3.

The above transformation equation for the acceleration case is limited in that it applies only to atoms which have a positive initial momentum. If the distribution includes atoms with negative initial momentum (e.g., as is the case for a thermal distribution) and if the accelerating potential is sufficiently strong, then these atoms will be turned around and will also strike the surface. In this case the total momentum distribution for atoms striking the grating surface can be written as

$$n_i(p_i) = \frac{n(\sqrt{p_i^2 - 2\Delta K}) + n(-\sqrt{p_i^2 - 2\Delta K})}{\sqrt{1 - 2\Delta K/p_i^2}}. \quad (5)$$

The negative part of the momentum distribution is thus folded over into the positive half-plane, which will further narrow the final distribution. This equation has no solutions for  $p_i^2 < 2\Delta K$ , and the physical meaning is that any atom is imparted a minimum amount of kinetic energy, so  $n_i(p_i) = 0$  for  $p_i^2 < 2\Delta K$ .

In the decelerating potential case,  $\Delta K < 0$ , so as noted earlier, we must first launch the atoms, that is, give them a momentum boost. This can be done in several ways, one of which is to hit the atoms with a short pulse of near-resonant light. This will give a launch momentum (boost) of  $p_L = N\hbar k$  where  $N$  is the average number of photons scattered per atom. This will also heat the atoms somewhat, so a better option is to use the ‘travelling molasses’ scheme [9] in which the atoms are cooled into a moving frame of reference. A third option is to turn on briefly a non-uniform magnetic field to produce a potential gradient, resulting in

$$p_L = \mathbf{F}_B \Delta t = g_F m_F \mu_B \nabla(B) \Delta t. \quad (6)$$

Whatever method is used, immediately after the launch, the initial atomic distribution  $n(p)$  is simply shifted over according to  $n_i(p_i) = n(p_i - p_L)$ . Subsequently the distribution is slowed as described before for a decelerating potential.

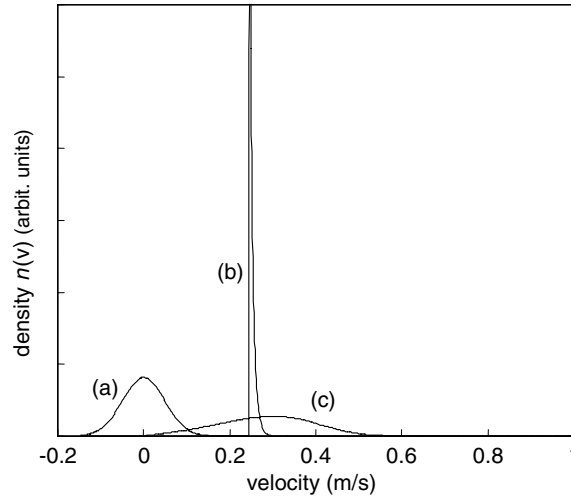


**Figure 4.** (a) An initial atomic thermal velocity distribution, with  $T = 25 \mu\text{K}$  and rms thermal speed  $v_T = 0.049 \text{ m s}^{-1}$ . (b) Distribution for atoms striking a grating surface after falling downwards a distance 3 mm. (c) Distribution for atoms striking the surface after launch upwards a distance 30 mm. Parameters were chosen for (b) and (c) such that in either case atoms with zero initial thermal speed arrive at the surface with speed  $5 v_T$ .

Now we will apply these results to a realistic momentum distribution. A MOT prepares atoms in a thermal distribution of one-dimensional momenta described by

$$n(p) = \frac{1}{p_T \sqrt{2\pi}} e^{-p^2/2p_T^2} \quad \text{where} \quad p_T = \sqrt{kT}. \quad (7)$$

If the atoms are dropped we can solve (5) to find the accelerated distribution

$$n_i(p_i) = \frac{1}{p_T \sqrt{2\pi}} \left( \frac{2}{\sqrt{1 - 2\Delta K/p_i^2}} \right) e^{-(p_i^2 - 2\Delta K)/2p_T^2}. \quad (8)$$

Examples of the original and accelerated distributions are shown in figure 4 as (a) and (b), respectively, for the specific case of atoms of  $^{85}\text{Rb}$  at a temperature of  $25 \mu\text{K}$ . Here we show the true velocity distributions taking into account the atomic mass. It is clear that there is a significant narrowing and a folding over of the distribution. The initial thermal distribution can be characterized by a full width  $\Delta p = 2p_T$  defined by the limits  $\pm p_T$ , this range containing about 68% of the atoms. Because the accelerated distribution has an unusual shape we characterize its width by mapping these limits onto the new distribution, knowing it will represent about 68% of the population. Due to the folding, the actual lower limit to the new distribution is due to atoms with initial momentum of 0, not  $-v_T$ , so the width is reduced by a factor of 2 beyond the acceleration compression. It can be shown that for large kinetic energy gain ( $p_T^2 \ll 2\Delta K$ ), the general expression for the width defined in this way is

$$\Delta p_i \cong \frac{p_T^2}{2\sqrt{2\Delta K}} \quad (9)$$

which decreases with increasing  $\Delta K$ . The typical momentum after falling is  $p_i \cong \sqrt{2\Delta K}$

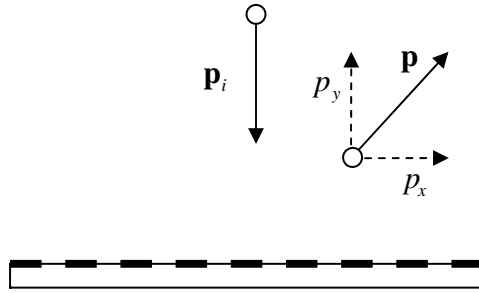


Figure 5. Momenta of incident and diffracted atoms.

so the relative width is

$$\frac{\Delta p_i}{p_i} \cong \frac{1}{2} \left( \frac{p_T^2}{2\Delta K} \right). \quad (10)$$

For the accelerated distribution in figure 4,  $\Delta p_i/p_i \cong 0.02$ .

Curve (c) in figure 4 shows the distribution obtained using the launch method into a decelerating potential ( $\Delta K < 0$ ), and the distribution is seen to be broadened, with  $\Delta p_i/p_i \cong 0.6$ . If the typical atomic momentum incident on the grating surface is much larger than  $p_T$ , then the momentum distribution width is

$$\Delta p_i \cong 2p_T \frac{p_L}{\sqrt{p_L^2 + 2\Delta K}} = 2p_T \left( \frac{s}{\sqrt{s^2 - 1}} \right) \quad (11)$$

where  $s \equiv p_L/\sqrt{2|\Delta K|}$  is a measure of the launch strength. The expression in brackets is always greater than 1 and signifies the broadening beyond the original thermal width,  $2p_T$ . This expression blows up for slow launch speeds ( $s \sim 1$ ) and decreases for fast launch speeds ( $s \gg 1$ ). Here the typical momentum is  $p_i \cong \sqrt{p_L^2 + 2\Delta K}$  so that

$$\frac{\Delta p_i}{p_i} \cong 2p_T \frac{p_L}{p_L^2 + 2\Delta K} = 2 \frac{p_T}{\sqrt{2|\Delta K|}} \left( \frac{s}{s^2 - 1} \right). \quad (12)$$

Finally we note that if there is no accelerating potential and the atoms are launched towards the grating,

$$\frac{\Delta p_i}{p_i} = \frac{2p_T}{p_L}. \quad (13)$$

### 3. Diffracted atom trajectories

Consider an atom arriving at the grating with incident momentum  $\mathbf{p}_i$  normal to the surface as shown in figure 5 and scattering off with momentum  $\mathbf{p}$  (components  $p_x$  and  $p_y$ ). We model the diffraction process as taking place within a thin layer of thickness  $\delta y$  near the surface. The size of  $\delta y$  depends upon the details of the atom–surface interaction, but we assume that it is small enough that the potential  $U(y)$  does not significantly affect the atomic motion during the diffraction process. This will be true if  $|\Delta U| \cong \left| \frac{dU}{dy} \delta y \right| \ll p_i^2/2$ . Note that  $U(y)$  excludes the potential caused by the grating. In this model the atoms are classical particles which emerge from the thin layer with momenta described by a probability distribution, which is itself dependent upon the incident momentum distribution and the details of the diffraction process.

Because we can neglect the external potential inside the thin layer, atoms emerge from it at initial angles given by  $\sin \theta = n\lambda/d = n\kappa/k$  where  $\kappa = 2\pi/d$  and  $k = 2\pi/\lambda$ .

The  $x$ -momentum of a diffracted atom is  $p_x = p \sin \theta = n\hbar\kappa$  and this is set by the grating spacing  $d$  and the order  $n$ , independent of the incident speed. In contrast, the vertical momentum after diffraction is  $p_y = \pm\sqrt{p_i^2 - p_x^2}$  (where we have used the fact that  $p^2 = p_i^2$  because it is an elastic collision) and so depends upon the incident speed. The location of the atom at a later time after it is far from the diffracting surface is determined by both  $p_x$  and  $p_y$ . If there is a strong accelerating potential  $U(y)$ , then  $p_y$  at later times is determined primarily by the potential, and the effect of the initial thermal momentum upon later position becomes very small. This effect is well known in charged particle optics [10]. If there is a horizontal detection plane (perhaps realized by a probe laser beam) a distance  $H$  from the grating, then the atom will cross the plane at the horizontal position

$$x = p_x t_H = n\hbar\kappa t_H \quad (14)$$

where  $t_H$  is the time to travel vertically the distance  $H$ .

If the potential is non-uniform then the general solution for the vertical position obeys

$$\ddot{y}(t) = -\frac{dU}{dy} \quad (15)$$

which can be solved for a given  $U(y)$  numerically. For a linear potential (e.g., gravity) we have the familiar solution

$$y(t) = y_G + p_y t - \frac{1}{2}\alpha t^2 \quad \text{where} \quad \alpha = \left| \frac{dU}{dy} \right| \quad (16)$$

and we choose our coordinates so that the  $y$ -acceleration  $a_y = -\alpha$  is always negative.

We solve for the travel time using  $H = y(t_H) - y_G$ ,

$$t_H = \frac{1}{\alpha} \left( \pm \sqrt{p_y^2 - 2\alpha H} + p_y \right) \quad (17)$$

where the choice of sign depends upon the detection geometry. The sign choices for  $p_y = \pm\sqrt{p_i^2 - p_x^2}$  are for a transmitting or reflecting grating, respectively. In most realistic cases we will have  $p_x^2 \ll p_i^2$  so we will approximate  $p_y \cong \pm p_i$ . For a reflection grating the  $x$ -position at time  $t_H$  is

$$x \cong (n\hbar\kappa/\alpha) \left( \pm \sqrt{p_i^2 - 2\alpha H} - p_i \right). \quad (18)$$

Because  $x$  depends upon  $p_i$  we expect that we may have chromatic dispersion in the diffraction fringes. We next apply these results to several particular experimental arrangements which are shown in figure 6.

#### Case (i): drop-bounce-fall back

In this situation, atoms are accelerated by the potential over a distance  $D$  and diffract upwards, then fall back to be detected by a probe laser beam as shown. We are interested in the later solution in time so the sign choice in (18) is positive. Noting that in this geometry  $p_i < 0$  we write

$$x = (n\hbar\kappa/\alpha) \left( \sqrt{p_i^2 - 2\alpha H} + |p_i| \right). \quad (19)$$

In general  $2\alpha H < p_i^2$  but  $2\alpha H$  is not necessarily negligible unless we intentionally choose  $H = 0$  in which case we have the simple expression

$$x = 2|p_i| n\hbar\kappa/\alpha. \quad (20)$$

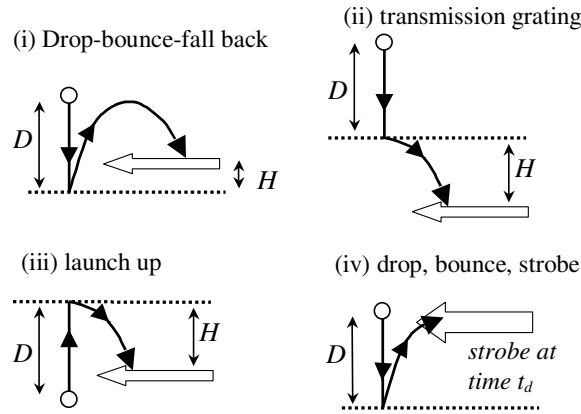


**Figure 6.** Several atom-diffraction geometries in which acceleration plays a significant role. Cases (i), (ii) and (iv) have been used in recent experiments.

Keeping to the general case  $H \neq 0$ , if the atoms are accelerated strongly,  $\Delta p_i/p_i \ll 1$ , so we can approximate

$$\Delta x \cong \frac{dx}{dp_i} \Delta p_i = (n\hbar\kappa/\alpha) \left( \frac{\sqrt{p_i^2 - 2\alpha H + |p_i|}}{\sqrt{p_i^2 - 2\alpha H}} \right) \Delta p_i \quad (21)$$

where  $\Delta x$  and  $\Delta p_i$  represent the widths of the distribution of atomic detected positions and incident momenta, respectively.

An important figure of merit for experimental resolving of diffraction is the relative spread, the ratio of width  $\Delta x$  to the separation of diffracted orders  $x_n - x_{n-1}$ . For this case,

$$\frac{\Delta x}{x_n - x_{n-1}} \cong n \left( \frac{\Delta p_i}{p_i} \right) \frac{1}{\sqrt{1 - H/D}} \quad (22)$$

where we have made use of the fact that  $p_i^2 \cong 2\alpha D$  for strong acceleration. Using our results from (10),

$$\frac{\Delta x}{x_n - x_{n-1}} = \frac{1}{2} n \frac{1}{\sqrt{1 - H/D}} \left( \frac{p_T^2}{2\alpha D} \right). \quad (23)$$

For the case of sub-Doppler laser-cooled atoms, the expression in brackets is small for drop distances of even a few millimeters. For best resolution we should choose large  $D$  and small  $H$ , and note that it is possible to use  $H < 0$ , in which case we should choose  $|H|$  large. This geometry was used in experiments with  $^{87}\text{Rb}$  atoms diffracting from an optical evanescent wave grating [5]. Using (23) and their stated conditions (1D atomic speed = 21 mm s<sup>-1</sup>,  $D \cong 18$  mm, and  $H \cong 12$  mm), the  $n = 1$  relative spread is about  $1 \times 10^{-3}$ .

#### Case (ii): a transmission grating

In this case atoms are dropped to the grating and pass through to a detection plane below. We note that this could also be accomplished using a reflection-type grating by applying a magnetic field with a gradient that accelerates the atoms into the grating, then reversing the field immediately after the diffraction so that the atoms accelerate away.

For the transmission grating case, the incident momentum is the same as in the previous case, but we must change the sign of  $H$ , and because it is transmission,  $p_y \cong + p_i$  so we must have

$$x = (n\hbar\kappa/\alpha)(\sqrt{p_i^2 + 2\alpha H} - |p_i|) \quad (24)$$

and the relative spread is

$$\frac{\Delta x}{x_n - x_{n-1}} \cong \frac{1}{2}n \frac{1}{\sqrt{1 + H/D}} \left( \frac{p_T^2}{2\alpha D} \right). \quad (25)$$

This is quite similar to the result for case (i). Here the resolution improves with larger values of  $H$  and  $D$ . The transmission geometry has been used for a double slit interferometer [11], which is similar to a transmission grating though with lower inherent resolution. In the experiment metastable neon atoms were cooled to about 2.5 mK using Doppler-cooling in a MOT. The atoms were allowed to fall 76 mm to a double slit and detected 117 mm below the slit by a channel electron-multiplier plate. Due to the relatively high temperature and the low atomic mass, the ratio  $p_T^2/2\alpha D \cong 0.70$ , so chromatic spread was actually quite significant, and (25), which for this large thermal momentum is only a rough approximation, gives a relative position spread for  $n = 1$  of about 0.22. In the actual experiment, time-of-flight selection was used to reduce further the effective  $\Delta p$  so that fringes could be resolved.

#### *Case (iii): launch up*

This method offers the advantage that the typical incident momentum can be made less than the drop momentum  $\sqrt{2\alpha D}$ . This may be desirable if the reflecting potential of the grating is small. In this geometry, the detection is below the grating and  $p_i > 0$  so

$$x = (n\hbar\kappa/\alpha) \left( \sqrt{p_i^2 + 2\alpha H} - p_i \right). \quad (26)$$

As mentioned, it is possible to have small incident momentum in this geometry, so we examine the special case that  $p_i^2 \ll 2\alpha H$  for which

$$x \cong (n\hbar\kappa/\alpha)(\sqrt{2\alpha H} - p_i) \quad (27)$$

where we keep only the leading term in  $p_i$  because that determines the dispersion, which is

$$\Delta x \cong (n\hbar\kappa/\alpha)\Delta p_i. \quad (28)$$

Using our earlier results for the launch momentum distribution, we find the relative spread

$$\frac{\Delta x}{x_n - x_{n-1}} \cong 2n \left( \frac{s}{\sqrt{s^2 - 1}} \right) \frac{p_T}{\sqrt{2\alpha H}}. \quad (29)$$

This expression applies to situations where the launch momentum  $p_L$  is chosen so that the incident momentum  $p_i \cong \sqrt{p_L^2 - 2\alpha D}$  meets the requirements  $p_T^2 \ll p_L^2 \ll 2\alpha H$ . If we compare to the previous two cases, assuming similar distances, the spread from (29) is significantly larger, as expected, because deceleration broadens the incident momentum spread.

#### *Case (iv): drop, bounce, detect with a flash strobe near peak*

Here the atoms fall, diffract upwards and are detected near their peak by briefly turning on an illuminating laser. With this method there is no well-defined detection plane, instead there is a well-defined detection time. At first glance, because  $x = p_x t = n\hbar\kappa t$ , we might expect that

a well-defined detection time would give zero dispersion in horizontal position. This is not, in fact, the case, because the time  $t$  here is measured from the moment of diffraction, but the atoms reach the surface at different times after release from the MOT due to their momentum spread. Thus we should more properly use  $x = n\hbar\kappa(t_d - t_i)$  where we have specified the detection time,  $t_d$ , and the time a particular atom is incident upon the surface,  $t_i$ . For an initial thermal momentum  $p_0$ ,

$$t_i = (1/\alpha)(\sqrt{p_0^2 + 2\alpha D} + p_0). \quad (30)$$

We have  $p_0^2 \ll 2\alpha D$  so

$$t_i \cong \sqrt{2D/\alpha} + p_0/\alpha \quad (31)$$

where we keep only the leading term in  $p_0$ . The obvious choice for detection time is at the peak of the bounce, calculated for atoms with zero initial velocity, which is  $t_d = 2\sqrt{2D/\alpha}$ . Then

$$x = n\hbar\kappa(t_d - t_i) \cong n\hbar\kappa(\sqrt{2D/\alpha} - p_0/\alpha). \quad (32)$$

So the position spread is  $\Delta x = n\hbar\kappa \Delta p_0/\alpha$  and using  $\Delta p_0 = 2p_T$ ,

$$\frac{\Delta x}{x_n - x_{n-1}} \cong 2n \frac{p_T}{\sqrt{2\alpha D}}. \quad (33)$$

This is similar to case (iii) but missing the deceleration broadening term. This method has been used with a corrugated magnetic reflector [12]. In this experiment, the order splitting was not large enough to be observed because of the non-zero source size, even with the advantage of a curved reflector for focusing [13]. Using (33) and the experiment's parameters of Rb atoms at 24  $\mu\text{K}$  and a 27 mm drop, we find the chromatic relative spread would be 0.13, which is significant. Note that the order splitting could be increased by using a finer diffraction grating, but the chromatic relative spread, which does not depend on  $d$ , would remain the same.

#### *Case (v): no external potential*

We can compare for reference to the case of no accelerating potential in which case the time to travel is simply  $t_H = H/p_y$  so that  $x = n\hbar\kappa H/p_y$ . If we use as we have been doing the approximation  $p_y \cong |p_i|$ , then we see that the spread of  $x$  values again depends upon  $p_i$  but in a more complicated way. We can express it reasonably simply as

$$\Delta x = n\hbar\kappa H \frac{\Delta p_i}{(p_L)^2 - (\Delta p_i)^2} \quad (34)$$

where we have made use of the fact that the launch momentum  $p_L$  is the median of the momentum range, true for any symmetric original momentum distribution but in particular for a thermal distribution. If  $(p_L)^2 \gg (\Delta p_i)^2$ , then the relative spread is

$$\frac{\Delta x_n}{x_n - x_{n-1}} \cong 2n \frac{p_T}{p_L}. \quad (35)$$

We see that in all of the above cases the relative spread increases with order  $n$ , and depends upon the ratio of the thermal momentum  $p_T$  to a characteristic momentum, such

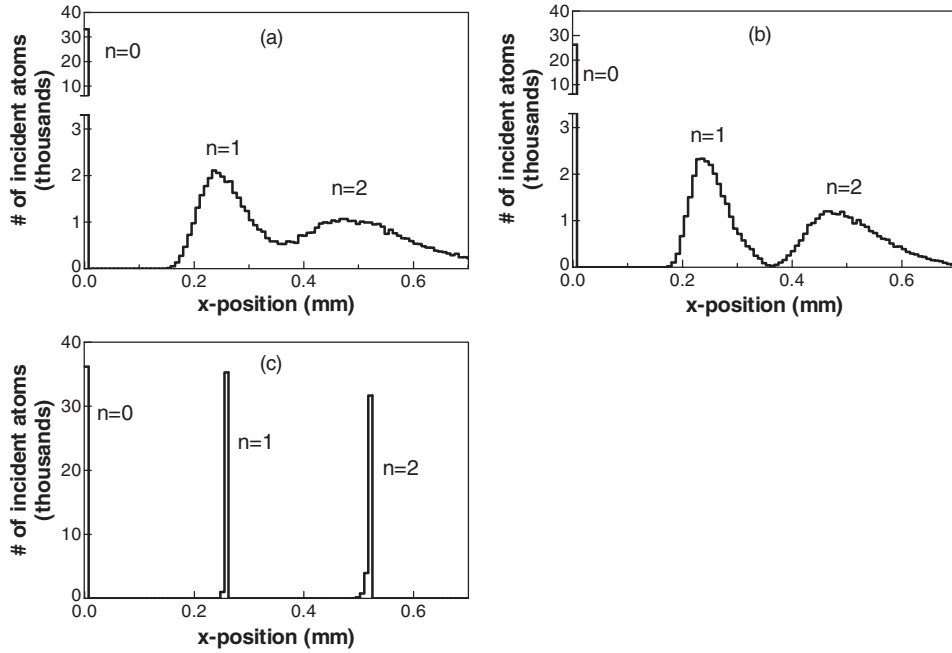


**Figure 7.** Simulations. (a) Diffraction of atoms launched at a reflection grating, with no accelerating potential. (Note the broken vertical axis.) (b) Diffraction of atoms launched upward at a grating, with a decelerating potential. (c) Diffraction of atoms accelerated through a transmission grating.

as  $\sqrt{2\alpha D}$  or  $p_L$ . Cases (i) and (ii) offer the best reduction in the relative spread for a given height.

#### 4. Atom diffraction simulation

We have explored three of these cases further by solving the equations of motion exactly for a thermal distribution of atoms. We chose conditions so that the median incident momentum was five times the  $25 \mu\text{K}$  thermal momentum, the same as for the Rb atomic distributions shown in figure 4. We send approximately  $10^5$  atoms at a diffraction grating with  $d = 1 \mu\text{m}$  and model the diffraction as simply scattering the atoms randomly with equal probabilities into the orders  $n = 1, 2$ , or  $3$ . Figure 7(a) shows the distribution of detected positions in our simulation for atoms launched towards a reflection diffraction grating, for the case where there is no external potential. The  $n = 0$  order is a delta function and the other orders show widths increasing with order number, as expected. Our model predicts a relative spread of  $0.40$ , which agrees well with the simulation. Figure 7(b) shows the results for a launch against gravity upward a distance  $D = 30 \text{ mm}$  at  $0.81 \text{ m s}^{-1}$  and detection at the original location ( $H = 30 \text{ mm}$ ). This gives the parameter  $s = 1.05$  and the broadening factor  $s/\sqrt{s^2 - 1} \cong 3.3$ . On the other hand,  $p_T/\sqrt{2\alpha H} \cong 0.064$ , so our model predicts a relative spread of  $0.42$ , very similar to the no-gravity case. Figure 7(c) shows the results for a transmission grating, in which the atoms fall under gravity a distance  $D = 3 \text{ mm}$  to the grating and a further distance  $H = 30 \text{ mm}$  to the detection plane. The combination of a narrowed incident momentum

distribution and acceleration afterward gives a dramatically reduced position distribution. Note the asymmetric peak shape, which is a result of the folded momentum distribution.

## 5. Conclusions

We have shown that the choice of experimental arrangement can aid in reducing the chromatic spread in diffraction patterns of cold atoms when there is an accelerating potential involved. We have found expressions for the relative position spread in detected atoms for several practical geometries and see that the resolution improves proportional either to the drop distance or the square root of the drop distance. We have applied our models to experimental situations used by several other researchers and expect our results may be of use in designing new experiments in cold atom optics.

## Acknowledgments

We thank J Shertzer for helpful comments on the manuscript. Financial support for this work was provided by grants from Research Corporation and the American Chemical Society.

## References

- [1] Peters A, Chung K Y and Chu S 1999 *Nature* **400** 849  
McGuirk J M, Foster G T, Fixler J B, Snadden M J and Kasevich M A 2002 *Phys. Rev. A* **65** 033608
- [2] Roach T M, Abele H, Boshier M G, Gahbauer F, Grossman H L, Zetie K P and Hinds E A 1996 Cold atom reflection from flat and curved magnetic mirrors *Proc. 12th Int. Conf. on Laser Spectroscopy* (Capri: Italy)
- [3] Aminoff C G, Steane A M, Bouyer P, Desbiolles P, Dalibard J and Cohen-Tannoudji C 1993 *Phys. Rev. Lett.* **71** 3083
- [4] Roach T M, Abele H, Boshier M G, Grossman H L, Zetie K P and Hinds E A 1995 *Phys. Rev. Lett.* **75** 629
- [5] Landragin A, Cognet L, Horvath G Z K, Westbrook C I, Westbrook N and Aspect A 1997 *Europhys. Lett.* **39** 485
- [6] Davis T J 2001 *Eur. Phys. J. D* **14** 111  
Davis T J 2001 *Eur. Phys. J. D* **14** 289
- [7] Sheehy B, Shang S-Q, Watts R, Hatamian S and Metcalf H 1989 *J. Opt. Soc. Am. B* **6** 2165
- [8] Chen H and Riis E 2000 *Appl. Phys. B* **70** 665
- [9] Clairon A, Salomon C, Guellati S and Phillips W D 1991 *Europhys. Lett.* **16** 165
- [10] de Wolf D A 1990 *Basics of Electron Optics* xvii (New York: Wiley) p 228
- [11] Shimizu F, Shimizu K and Takuma H 1992 *Phys. Rev. A* **46** R17
- [12] Rosenbusch P, Hall B V, Hughes I G, Saba C V and Hinds E A 2000 *Phys. Rev. A* **61** 031404
- [13] Saba C V, Barton P A, Boshier M G, Hughes I G, Rosenbusch P, Sauer B E and Hinds E A 1999 *Phys. Rev. Lett.* **82** 468